Rotational distributions of excited CN molecules following electron- and photon-stimulated desorption from surfaces

Jun Xu,* Alan Barnes, Royal Albridge, Carl Ewig,† and Norman Tolk
Department of Physics and Astronomy, Vanderbilt University, Nashville, Tennessee 37235

Lester D. Hulett, Jr.
Oak Ridge National Laboratory, P.O. Box 2008, MS 6142, Oak Ridge, Tennessee 37831-6142
(Received 29 June 1992; revised manuscript received 26 April 1993)

We report systematic experimental studies of rotational distributions of excited CN desorbed from alkali-metal and alkali-metal-halide surfaces following excitation by incident photons and electrons. Newly measured rotational spectra are found to exhibit temperature-independent non-Boltzmann features that are uniquely correlated to the particular alkali-metal component of the substrate. In addition, we observe that photon-excitation functions and cross sections for CN^* desorption also depend strongly on the alkali-metal component of the substrate. The data reveal that rotational distributions arising from electron-stimulated desorption (ESD) and photon-stimulated desorption (PSD) are markedly different from those seen in thermal desorption and molecule-surface scattering. The marked substrate dependence of the rotational distributions indicates that molecular-rotation distributions following ESD and PSD are determined by direct electronic bond breaking and reflect the nature of the potential-energy surfaces that characterize CN–alkali-metal interactions. Utilizing the measured rotational distributions in conjunction with a hindered rotor model, we have constructed angular-dependent potential surfaces.

I. INTRODUCTION

In studies of bond making and breaking on surfaces, it is important to identify and characterize the contributing dynamical mechanisms and as much as possible to elucidate the role of potential surfaces in these processes. Desorption of surface constituents induced by electronic transitions (DIET), specifically electron- or photon-stimulated desorption (ESD and PSD), constitutes a useful tool for treating this problem. Recent studies on rotational and vibrational distributions of desorbed molecules have been carried out to investigate desorption mechanisms.[1–4] For all adsorbed molecules, interaction potentials are functions of the angle between the surface normal and the molecular axis as well as of the reaction coordinate, defined as the distance between desorbate and the surface. Many experimental and theoretical studies have been carried out with emphasis on the reaction coordinate.[5] In contrast, although there are some theoretical treatments, there are few experimental data regarding the role of the angular dependence of the interaction potential in electronic desorption. On the theoretical side, Gadzuk and co-workers[6,7] proposed a model for thermal desorption to relate the angular dependence of the ground-state potential surface to rotational distributions of desorbed molecules. The model is based on an approximation that the hindering potential surface is suddenly switched off as the adsorbed molecule promptly leaves the surface. This approximation is assumed to be valid for the case of electronic cleavage of strongly bound molecules. Burns, Stechel, and Jennison[8] developed a picture that describes ESD of NO molecules emitted in the ground state. In their model, as the adsorbate is excited from a hindered-rotor to a free-rotor state, some rotational angles result in an antibonding reaction-coordinate-dependent potential leading to desorption. Recently, some theoretical works by Hasselbrink[9] and also Krempl[10] have attempted to relate the angular dependence of the repulsive-state potential surface to the rotation of ejected molecules.

Measurements of internal energy distributions constitute a powerful tool in understanding the dynamics of molecular interactions with surfaces. In thermal molecular-desorption experiments, the resulting rotational distributions are observed to have a temperature-dependent Boltzmannlike character.[11,12] In surface-molecule scattering experiments, rotational distributions of scattered molecules are found to be distinctly non-Boltzmann, to vary only weakly with surface temperature and to depend strongly on the incident energy and angle.[13–15] Rotational distributions arising from ESD and PSD have been exploratively observed to be non-Boltzmann in the NO-metal system under electron[1] and laser[2–4] bombardment. However, in stimulated desorption experiments, there have been up to now no measurements of the dependencies of the rotational distributions on substrate, temperature, and incident energy. These dependencies are important in elucidating the underlying mechanisms by which molecules acquire rotational motion following desorption induced by electronic transitions.

In this work, we studied electron- and photon-stimulated desorption of CN emitted in excited states from alkali-metal-halide and alkali-metal surfaces. Emphasis was on the measurements of rotational distributions (in ESD and PSD), photon-excitation functions, and

ESD cross sections. The rotational distributions following ESD and PSD are observed to be markedly different from the features observed either in thermal desorption or in molecule-surface scattering. These excited-state distributions are found to be independent of temperature and incident energy, and systematically correlated to the alkali-metal component of the substrate. This unique dependence of rotational distribution on substrate provides information on important aspects of molecule-surface interactions including potential-surface structure and the dynamics of bond breaking on surfaces.

II. EXPERIMENT

A detailed description of the experimental setup appears in Ref. 16. The work was carried out in an ultrahigh-vacuum (UHV) system, which operates at a base pressure of 1.0×10^{-10} Torr. To obtain surface CN adsorbates,[16,17] gases were admitted to the chamber through two Varian leak valves allowing the partial pressures of two gases, CO_2 and N_2, to be controlled in the range of 1.0×10^{-10} to 1.0×10^{-6} Torr. The incident radiation is either electrons or synchrotron radiation. Optical emissions arising from bulk fluorescence or/and desorbed excited species under the radiation were imaged onto the entrance slit of a McPherson 0.3-m monochromater (model 218). Photons were detected by a cooled photomultiplier, operated in a pulse counting mode. The stepping motor grating control and scaler for photon counting were interfaced through CAMAC and IEEE-488 to an Apple MacIntosh computer.

Electrons were produced from a gun built from the design of Stoffel and Johnson[18] operated in the energy range 60–900 eV at typical currents of 1–500 μA. The spot size at the sample was about 2 mm in diameter for the ESD measurements. The PSD measurements were carried out at the University of Wisconsin Synchrotron Radiation Center (SRC) using the Vanderbilt/SRC joint beam line. Figure 1 illustrates the schematics of the beam line, which consists of a 6-m toroidal grating monochromator (TGM) which delivers dispersed light in the range from 9–190 eV and, at zero order, undispersed synchrotron light. The photon-beam spot in the sample plane was 2.7-mm high by 7-mm wide. In order to reduce the amount of second-order light, tin, indium, and LiF filters were used. An aluminum foil was used to block the visible or uv lights from the beam line for the undispersed light experiments. A 93% transparent nickel mesh was mounted in the beam line and used to measure the beam flux.

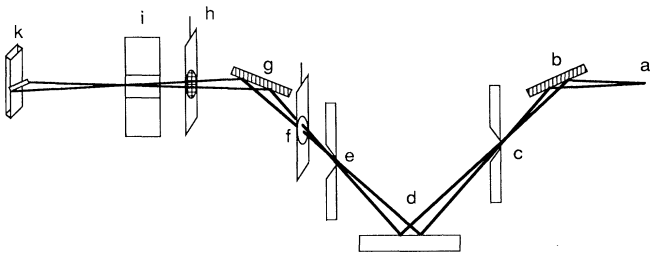

FIG. 1. Schematic of 6-m TGM Vanderbilt/SRC beam line in Synchrotron Radiation Center. (a) Synchrotron source, (b) entrance mirror, (c) entrance slit, (d) toroidal-grating monochromator (TGM), (e) exit slit, (f) filters, (g) exit mirror, (h) Ni or Au mash, and (i) differential pump.

The alkali-metal halide crystals were cleaved in air, mounted on a micromanipulator with their (100) surfaces facing the beam, and heated under UHV conditions for cleaning. Thick alkali-metal layers were obtained by evaporation from alkali dosers (SAES) onto glass slides. It is difficult to measure Auger emissions because of the charging effects produced by electron bombardment of the insulators. However, we used optical emissions to characterize the surfaces. When a surface was cleaned, the optical emissions were observed to be contributed to the bulk fluorescence and desorbed excited atoms which are the constituents of the substrates. As we exposed the surface to gaseous molecules, optical emissions were observed to arise from desorbed excited atoms and molecules which are related to the gaseous molecules. For the PSD measurements the sample temperature could be varied between room temperature and 800 K. For the ESD experiments the samples are in thermal contact with a close cycle helium cooler which can control the sample temperature from 50 to 350 K.

Precise measurements of rotational spectra require the spectrometer to have high resolution and to be well calibrated. A 2400-lines/mm grating with 3000-Å blaze was used to measure high-resolution spectra with 30-μm slits. Our wavelength calibration was obtained by using an iron-discharge source. Results show that deviation between experimental wavelengths and true wavelengths exhibit a *sine* function with a period of 25 Å and amplitude of 0.103(7) Å due to error in machining of the central driving screw which was approximately sinusoidal. This error was corrected in the data analysis.

III. FEATURES OF THE CN EMISSION

A. Generation of excited CN emission

Bombardment of alkali-metal halide surfaces with low-energy electrons and with synchrotron photons produces optical emissions which arise from (a) desorbed excited molecules and atoms, (b) excited bulk impurity, and (c) defect recombination in the bulk materials (bulk luminescence). Detection of optical emissions[19] possesses advantages including the ability to probe excited neutral desorbates, as well as defect processes in the bulk. Since it is difficult to characterize insulator surfaces by traditional methods such as Auger electron spectroscopy and low-energy electron diffraction, we use optical spectroscopy to characterize the surfaces. After a LiF sample was heated and annealed at 550 °C, the measured optical spectrum is found to be attributed to two features: (1) bulk fluorescence of the LiF substrate and (2) desorbed excited lithium atoms. There are no other emissions observed which arise from surface impurities. Then we exposed the LiF surface to gaseous H_2, H_2+CO_2, N_2+CO_2, or CO_2 for preparation of the surface with con-

tamination. Consistent with the exposure, we observed emission lines which are attributed to desorbed H* for the H_2 exposure, desorbed OH* for H_2+CO_2 exposure, desorbed CN* for N_2+CO_2 exposure, and desorbed CO* for CO_2 exposure, respectively. These exposure-associated emissions are dependent on the amount of the exposure. The original emissions associated with the clean surface conditions are reduced. This variation of the optical spectra indicates alternations of the surface conditions. Similar variations were observed for the other substrates discussed. The optical emissions give not only the surface impurities but also the molecular nature of the impurities. Although this optical method in characterizing surfaces is hindered by the limited ability in wavelength detection, we believe that optical spectroscopy is a valuable tool for insulator surface characterization.

The generation of excited CN molecules electronically desorbed from alkali-metal-rich surfaces is described in more detail in Ref. 16. CN* emission was identified from emissions of electron-bombarded LiF surfaces.[20] In our previous experiments,[16,17] we found that the desorbing CN molecules are generated through the following sequence: (a) pre-irradiation of alkali-metal halide crystal produces alkali-metal-rich surfaces, (2) surface CN molecules are formed when the alkali-metal-rich surface is exposed to CO_2 and N_2, and (3) electron or photon bombardment induces the desorption of excited CN molecules from the surface. To briefly illustrate the generation of CN* emission, Fig. 2 displays a set of optical spectra arising from 300-eV electron bombardment of a KCl surface at 60 K which was exposed to gaseous CO_2+N_2 at different exposure levels before electron irradiation. Initially a freshly cleaved KCl surface was pre-irradiated by the electrons *in situ* for 12 h at 80 μA. Under these conditions, it is well documented that electron[21–23] bombardment of alkali-metal halide substrates produces alkali-metal-rich surfaces. During this pre-irradiation there was no externally initiated gas exposure. Figure 2(a) shows the optical emission spectrum before exposure to CO_2 and N_2. Next, the pre-irradiated surface was exposed to 13 Langmuir (1 L$=1\times10^{-6}$ Torr s) of gaseous CO_2+N_2 (1:1). The resulting spectrum, Fig. 2(b), shows a feature at 3870 Å which we have identified as the $B^2\Sigma^+\rightarrow X^2\Sigma^+$ electronic transition in the desorbed excited CN radical. Figure 2(c) shows the optical emission spectrum from an electron-bombarded surface which has been pre-exposed to 96 L of gaseous CO_2+N_2 (1:1). The intensity of the characteristic line is markedly enhanced by this exposure. This intensity has been observed to saturate for exposures larger than about 200 L. This method to obtain surface CN adsorbates is similar to that described by Watanabe and co-workers.[24,25]

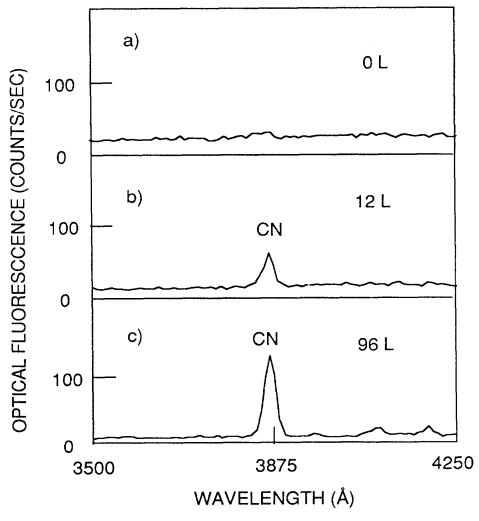

FIG. 2. Optical emission spectra due to 300-eV electron bombardment (a) on a clean KCl surface at 60 K, (b) on the surface with 12-L CO_2+N_2(1:1) exposure, and (c) on the surface with 96-L CO_2+N_2(1:1) exposure.

B. Alkali-metal correlation of CN* desorption decay

When the surface is prepared by CN coverage, electron-induced desorption removes the accumulated adsorbates from the surface leading to a decrease in the concentration of the adsorbate and consequently to a decrease in the desorption yield. The measurement of the dependence of this concentration on the substrate can provide information on the substrate dependence of the total cross section. It has been observed that the CN* ESD yield decreases as the electron beam bombards the CN-condensed surface, as shown in Fig. 3. Plotted is CN* desorption yield, normalized to the initial yield, as a function of electron dose during electron irradiation at 300-eV electron energy. Electron currents are 110 μA for KBr, 106 μA for KCl, 120 μA for NaCl, 118 μA for NaF, and 70 μA for LiF. We assume that the desorption yield is proportional to the surface CN concentration. Then the measured yield reflects the surface CN concentration. The decrease of the desorption yield represents the decrease of the surface concentration due to

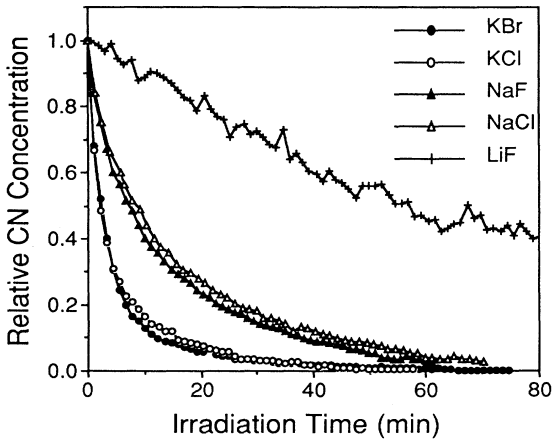

FIG. 3. Decay curves of the CN* desorption yield vs electron-beam dose. Background yields attributed to residual gas exposure were subtracted from the measured yields.

electron-induced CN desorption.

We define a total cross section for reducing the surface CN concentration. This reduction includes excited CN desorption, ground CN desorption, dissociation of adsorbed CN, and any other process which causes the reduction of surface CN concentration. The total cross sections were determined from our data in the following manner. The time rate of change of the surface CN concentration is proportional to the amount present on the surface and the incident electron flux (I/qA):

$$\frac{dN_{\mathrm{CN}}(t)}{dt} = -\sigma_T N_{\mathrm{CN}}(t)\left[\frac{I}{qA}\right], \tag{1}$$

where $N_{\mathrm{CN}}(t)$ is the number of surface CN molecules at time t, I is the incident electron current in amps, q is the electronic charge in Coulombs, A is the area of the incident electron-beam spot, and the constant of proportionality (σ_T) is the total cross section for reducing surface CN concentration. The solution of Eq. (1) shows that the amount of the surface CN decays exponentially and that the decay depends on the total cross section. The area of the beam spot is $A = 7.0\times10^{-2}$ cm^2 ($\pi 1.5^2$ mm^2). The total cross sections under 300-eV electron bombardment of alkali-metal halide surfaces are obtained by a nonlinear least-squares fit of the decay data shown above in Fig. 3 to an exponential function. The total cross sections are derived for LiF, NaF, NaCl, KBr, and KCl, as $(3.3\pm0.7)\times10^{-20}$, $(7.2\pm1.1)\times10^{-20}$, $(8.1\pm1.3)\times10^{-20}$, $(12.2\pm2.9)\times10^{-20}$, and $(14.4\pm2.7)\times10^{-20}$ cm^2, respectively. The errors are the relative errors derived from the least-squares fit.

It is obvious from Fig. 3 that the total cross section for reducing CN concentration under electron bombardment depends systematically on the alkali-metal component of the alkali-metal halide substrate, and is independent of the halide component. A higher atomic-number alkali metal (potassium) gives a larger cross section than a lower atomic-number alkali metal (lithium). This measurement indicates that there is a definite correlation between the presence of surface alkali metal and electron-induced removing of surface CN. Besides this global correlation, a detailed examination of Fig. 3 shows that decay curve is not exactly one exponential. This deviation may be due to the contributions from other processes such as carbon or/and nitrogen ESD or due to the assumption that the CN* ESD yield is not proportional to the surface CN concentration.

As shown in Fig. 3, the surface CN concentration decreases to almost zero under electron bombardment when there is no substantial exposure of the surface to the gaseous molecules. In our measurements of photon-energy dependencies and rotational distributions, it requires that the CN desorption yield is not a function of time. To meet this requirement, we dosed CO_2+N_2(1:1) at a constant pressure for the measurements. As described in Ref. 16, at a constant pressure of gas dose, it has been found that the CN* desorption yield grows as a function of the dosing time and that the growth tends to saturate at a level characteristic of the pressure. The saturation yield is understood as a balance between the desorption and formation.

C. Photon-excitation functions

The incident photon-energy dependence at room temperature of desorbing CN* was acquired using the low-energy gratings of the 6-m TGM. The yields arising from KCl and potassium-metal surfaces are displayed in Figs. 4(a) and 4(b). The excitation functions of desorbed CN* exhibit two resonant thresholds centered around 16 eV and 20 eV for both surfaces. Besides these resonances, there is a continuous-energy dependence of CN* desorption yield in the range of <7.8 to 30 eV.

To avoid the contribution to this signal by incident photons of second or higher orders, a tin-foil filter (1500-Å thick) was inserted into the path of the incident beam. This filter passes only first-order light according to the empirically determined transmission function. This reduces the incident flux by almost one order of magnitude. Since the fluorescence is very weak, each spectrum in Fig. 4 took about 4 h. The energy-dependent yields of CN* desorbed from KCl and the metal are normalized to the relative flux transmitted by this filter. The TGM entrance and exit slits are equally set at 1000 μm, which gave incident light resolution of 0.01 eV in full width at half maximum (FWHM).

Figure 4(c) shows the photon-energy dependence of CN* desorbed from a lithium-metal surface.[17] This photon-excitation function also shows two resonance structures: 16 and 22 eV. The lower-energy peak (16 eV) is the same as that observed for CN* desorbed from potassium-related surfaces. The higher-energy resonance

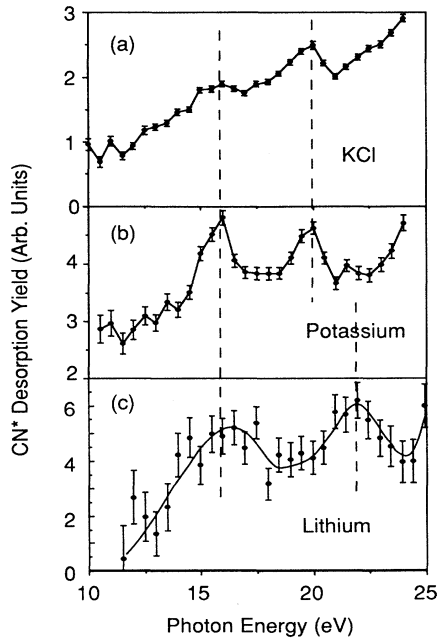

FIG. 4. Desorption yields of excited CN from (a) KCl, (b) potassium-metal, and (c) lithium-metal surfaces as a function of incident photon energy and normalized to incident photon flux. The CO_2+N_2(1:1) dose pressures are 2×10^{-7} Torr.

(22 eV) is shifted from the 20-eV resonance observed for CN* desorbed from potassium surfaces.

IV. MEASUREMENTS OF ROTATIONAL DISTRIBUTIONS

A. Substrate dependence

Figure 5(a) shows the R and P branches of the $B \rightarrow X$ transition of CN* desorbed from alkali-metal surfaces under 400-eV electron bombardment at a temperature of 60 K. The peak intensities relate to the population distribution of the CN $B^2\Sigma^+(v=0)$ rotational states. For lithium-, sodium-, potassium-, and cesium-metal surfaces, resolutions are 0.56, 0.59, 055, and 0.61 Å, respectively, in FWHM. The spectrometer was calibrated before and after each rotational spectrum at the same conditions. Similar rotational spectra were measured for alkali-halide substrates with 400-eV electrons and 60-K substrate temperatures, as shown in Fig. 5(b). For LiF, NaCl, KBr, and CsI surfaces, respectively, resolutions are 0.62, 0.54, 0.52, and 0.55 Å in FWHM.

We have analyzed the spectra by a least-squares fit procedure to determine rotational populations. The measured wavelength range covers the $B^2\Sigma^+ \rightarrow X^2\Sigma^+$ 0-0 and 1-1 transitions of CN molecules. We express the measured fluorescence intensity as

$$I(\lambda)=N^0\left\{\sum_J \nu^3 P^0(J)N(J)g[\lambda,\lambda_p(J)] + \sum_J \nu^3 R^0(J)N(J)g[\lambda,\lambda_r(J)]\right\} + N^1\left\{\sum_J \nu^3 P^1(J)N(J)g[\lambda,\lambda_p(J)] + \sum_J \nu^3 R^1(J)N(J)g[\lambda,\lambda_r(J)]\right\} + k\lambda + B_0 , \quad (2)$$

where $\lambda=\lambda_m-\delta(\lambda_m)$, λ_m is the measured wavelength, and $\delta(\lambda_m)$ is the deviation of the measured wavelength from the true wavelength, which has been measured to be a *sine* function with a period of 25 Å and amplitude of 0.103(7) Å due to errors in the machining of the central driving screw, k and B_0 are the noise parameters. $g[\ ]$ is the Gaussian shape of instrument resolution function, which was determined experimentally from the observed line shape of the mercury 4077-Å line. ν is the transition frequency. $\lambda_p(J)$ and $\lambda_r(J)$ are the transition wavelengths of the P and R branches, respectively. $P^0(J)$, $R^0(J)$, $P^1(J)$, and $R^1(J)$ are the rotational line strengths of the P and R branches, respectively (0 and 1 superscripts indicate the vibrational states). N^0 and N^1 are the vibrational population in $v=0$ and 1 states, respectively. $N(J)$ is the rotational population in state J. ν, $\lambda_p(J)$, $\lambda_r(J)$, $P^1(J)$, and $R^1(J)$ are determined by gaseous molecular spectroscopy.[26,27] References 26 and 27 also provide the spectroscopic constants, such as the band spectral region, the rotational constants, and the centrifugal distortion constants (excluding the small spin splitting), essential for calculation of the line positions. The least-squares fit determines the rotational and vibrational populations.

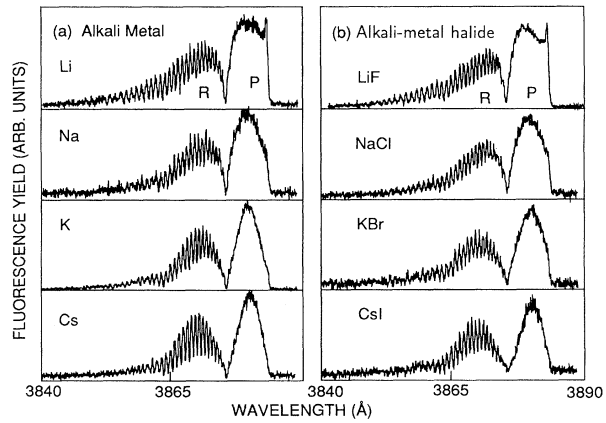

FIG. 5. P branches and rotational resolved R branches of $B^2\Sigma^+(v=0)\rightarrow X^2\Sigma^+(v=0)$ transition of CN* desorbed, respectively, (a) from alkali-metal surfaces and (b) from alkali-metal halide surfaces under 400-eV electron bombardment at 60 K. The CO_2+N_2(1:1) dose pressures are 2×10^{-7} Torr.

In Eq. (2), we assumed that the rotational populations in the $v=1$ state are the same as those in the $v=0$ state. Textbooks show that the P branch of the $v=1$ system overlaps the R branch of the $v=0$ system starting at $J=5$ but has no overlap with the $v=0$ P branch. In our fitting, the P and R branches were fitted simultaneously and the resulting residuals showed no systematic effects in the region of the $v=0$ P branch which would be distorted if the P branch of the $v=1$ system was significantly different from our assumption.

The fitted rotational distributions of desorbed CN* are plotted in Figs. 6(a) and 6(b), respectively, for alkali-metal halide and alkali-metal substrates. The plots are normalized to have an equal area. The average rotational energy $[\Sigma E(J)N(J)/\Sigma N(J)]$, the population width (full width of 10% maximum), and the relative vibrational population (N^1/N^0) are determined by the fit and listed in Table I. The results show quantitatively that the rotational distributions of desorbed CN* from alkali-metal halide surfaces are the same as those from the corresponding alkali-metal surfaces within experimental error and that rotational distributions strongly depend on substrates: substrates with a low alkali-metal atomic number showing a wider population than substrates with a high alkali-metal atomic number. The χ-squared rotational distributions of CN* desorbed from LiF and lithium-metal surfaces is 49 for 31 degrees of freedom indicating that the distributions are close but probably not exactly the same. The rotational distributions for lithium substrates are markedly different from those for cesium substrates. The χ-squared rotational distributions of CN* desorbed from LiF and CsI surfaces is 1062 for 23 degrees of freedom indicating the statistical impossibility of the two data sets coming from the same underlying distribution.

The above data indicate that rotational distribution of CN* desorbed from alkali-metal and electron-irradiated alkali-metal halide surfaces is independent of the halide component of the alkali-metal halide substrate. This indication is also verified by the distributions for KCl and KBr surfaces: the distributions have been measured to be

TABLE I. Average rotational energy, full width of 10% maximum, and relative vibration population as a function of substrate.

Substrate	$\langle E_r \rangle$ (eV)	Width ($\hbar$)	N^1/N^0 (%)	Substrate	$\langle E_r \rangle$ (eV)	Width ($\hbar$)	N^1/N^0 (%)
Li	0.041	28	7.7	LiF	0.040	26	7.4
Na	0.032	24	7.0	NaCl	0.031	23	7.0
K	0.028	21	10.2	KBr	0.029	20	10.2
Cs	0.029	20	13.0	CsI	0.029	19	13.0

similar to each other.

We have tested the reproducibility of our measurements and the validity of the errors assigned on the basis of the fit by comparing results from two runs taken on NaCl. The data were fit as described above. The individual rotational populations for the two runs were subtracted and normalized by the errors determined from the fit. The sum of the squares of these should be distributed according to a χ-squared distribution. The resulting χ square for this test was 22 for 29 degrees of freedom.

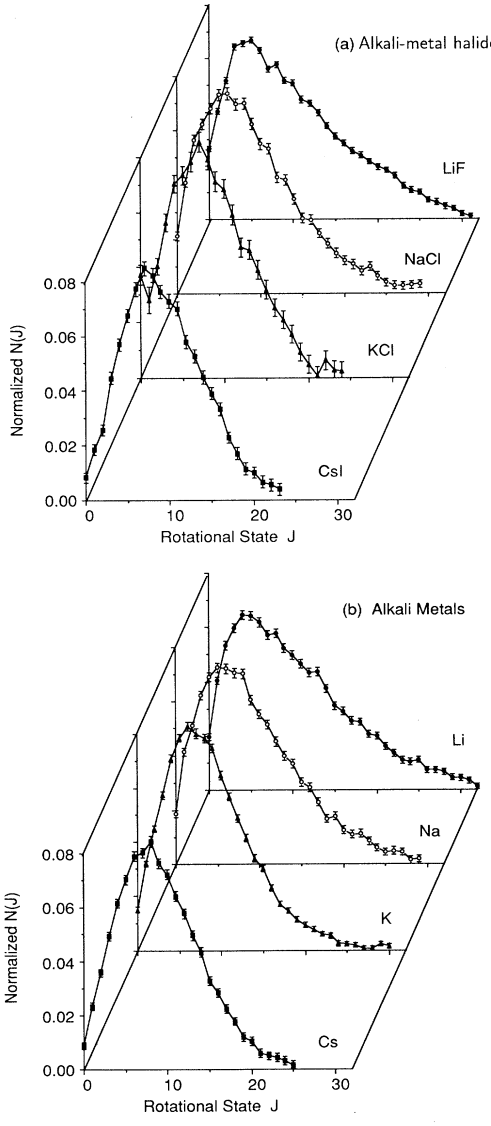

FIG. 6. Linear plots of rotational-state populations of CN* desorbed from (a) alkali-metal halide and (b) alkali-metal surfaces under 400-eV electron bombardment at 60 K.

B. Substrate temperatures

Figure 7 consists of Boltzmann plots of rotational distributions of CN* desorbed for lithium-metal and LiF surfaces as described in Fig. 6. The plots not only show a uniting of the distributions for the two lithium-associated substrates but also clarify that the plots are curved, not a straight line. If the emission of diatomic molecules follows thermal desorption, the Boltzmann plot of rotational distribution will be a straight line[11,12] and the rotational temperature depends on the surface temperature (they may not be equal). For comparison, a simulated Boltzmann distribution at 60 K, which is the substrate temperature we had, is plotted in the figure. The measured distributions are obviously in contrast to the simulation. The average rotational energy is 0.0408 eV which is equivalent to 482 K ($\langle E_r \rangle / K$). This is seven times above the surface temperature.

Figure 8 shows rotational distributions of desorbing CN* from a NaCl surface at two surface temperatures: 60 and 160 K. Electron energy was 400 eV at a current of

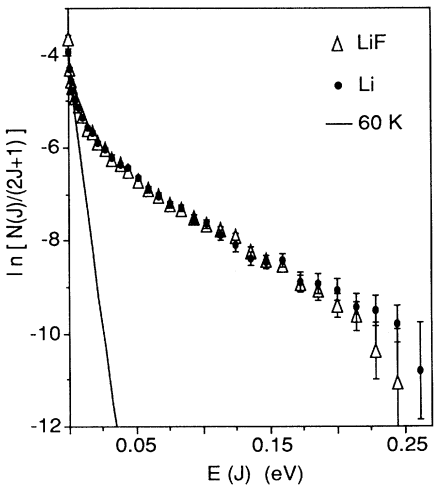

FIG. 7. Boltzmann plots of rotational distributions of excited CN desorbed from LiF (open triangle) and lithium-metal (filled circle) under 400-eV electron bombardment at 60 K. Line is the simulated Boltzmann distribution for 60 K.

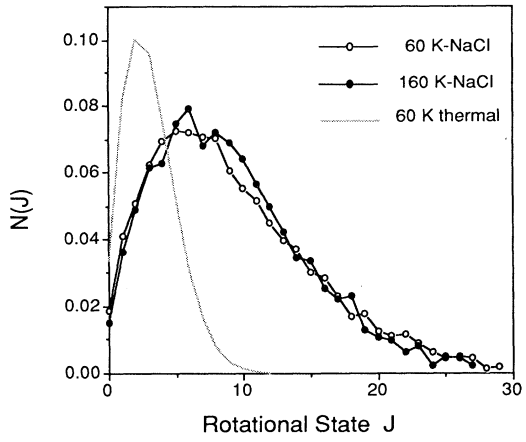

FIG. 8. Linear plots of rotational-state populations of CN* desorbed from NaCl for 60- and 160-K substrate temperatures. The weak line is the simulated Boltzmann distribution for 60 K.

about 150 μA. The data obtained showed no differences for different substrate temperatures. Similar results were obtained for other substrates which indicate that rotational distributions of desorbed CN* following ESD are independent of surface temperature in the range 60–300 K. These results are in contrast with those obtained for thermal-desorption experiments where the rotational distributions are very sensitive to substrate temperature.

C. Rotational distributions arising from PSD

Rotational distributions of desorbing CN* from a KCl surface have been measured for two electron energies: 150 and 400 eV at 60 K. The measurements show that there are no differences observed between the two spectra to within experimental error. This is very different from processes based on momentum transfer where incident energy is crucial in determining the rotational states of the scattered or sputtered molecules.

Rotational distributions have been measured for CN* desorbed from KCl and potassium-metal surfaces under synchrotron radiation at room temperature, as shown in Figs. 9(a) and 9(b). The rotational distributions in PSD from KCl and potassium-metal surfaces are not only close to each other but also close to those in ESD from KCl, KBr, and potassium-metal surfaces. It appears that the rotational distributions of desorbed CN* are identical for all potassium-related surfaces, independent of the radiation source and surface temperature.

As stated above, rotational spectra of desorbing CN* are very difficult to detect even for a zero-order synchrotron light beam. For first-order light, the incident flux is reduced by one-and-a-half orders of magnitude as compared to the zero-order light. A spectrum was measured for 20-eV photon beam as shown in Fig. 9(b). The resolution is 0.68 Å in FWHM. It seems that there is no obvious difference that we can see. Since the spectra have poor resolution, no fitting data are obtained.

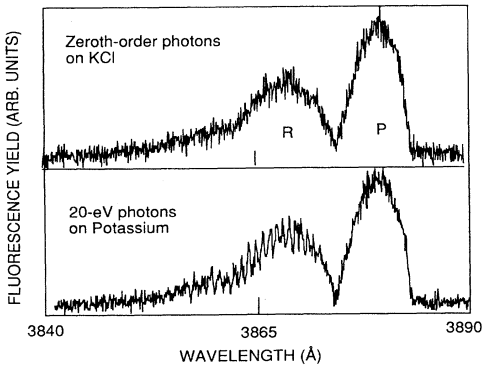

FIG. 9. Rotational spectra of excited CN desorbed from KCl surface under zero-order synchrotron light bombardment and from the potassium surface under 20-eV photon bombardment.

V. DISCUSSION

A. Desorption mechanisms

The photon-energy-dependent structure of desorbing CN* shows no systematic correlation with core-level excitation energies of either alkali metals or KCl. Instead, the data suggest that the mechanism responsible for CN* desorption is a direct electronic transition from a bonding state to an antibonding state of the surface bond, which is consistent with many features predicted by a Menzel-Gomer-Redhead model.[28,29] This transition is schematically illustrated in Fig. 10, which plots interaction potentials as functions of the distance between the center of mass of the CN molecule and the surface. An important question is the nature of the bonding and antibonding states participating in the observed desorption of excited CN in the *B* state.

Our experimental results clearly show that rotational distributions, desorption cross sections, and photon-

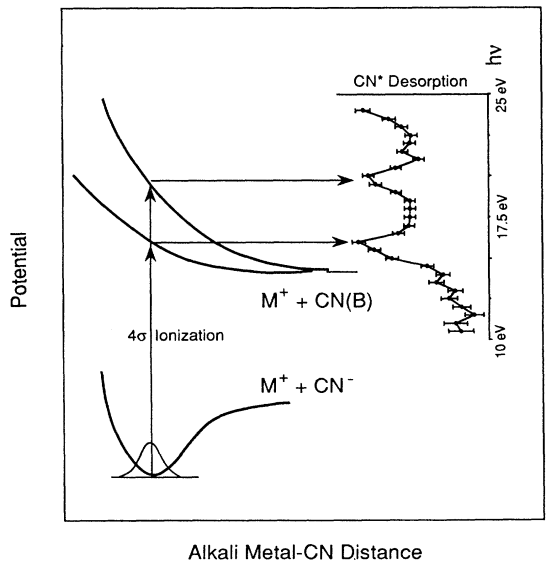

FIG. 10. Scheme of the one-dimensional Franck-Condon model for the desorption of CN* from surfaces.

excitation functions correlate systematically to the alkali metal not only for alkali metal but also for alkali-metal halides. In addition, it is well documented that alkali-metal halide surfaces become metalized under electron and photon bombardment. Based on these facts, we propose that the parent bond of desorbing Cn* is the bond between CN and the alkali-metal surface. Similar to gas-phase alkali-metal CN (Ref. 30) and to CN^- impurity in alkali-metal halide lattices,[31] the alkali-metal CN surface bond is believed to be an ionic bond due to the high electron affinity of CN neutral and the low ionization energy of the alkali metal. This strong Coulomb-attraction bond is likely to be the initial ground-state bond in the electronic transition leading to desorption.

Electron or photon bombardment supplies energy to the parent bond leading to the emission of CN on the B excited state. We observed a resonance peak at 16 eV in the photon-energy-dependent yield of desorbing CN* from KCl, potassium-, and lithium-metal surfaces. Theoretical calculations[32] show that the ionization energy from the adsorbed CN^- 4σ state in the Ni-metal CN system is 17 eV, which is close to our observed value for the alkali-metal CN system. The 4σ ionization of ground-state CN^- will result in an excited neutral CN in its B state and, hence, we believe that the 4σ ionization of the (alkali metal)$^+$-CN^- system produces an (alkali metal)$^+$-CN(B) cationic state. This state is likely to be strongly repulsive because of the absence of the original Coulomb attraction; thus the desorption of CN in the B state results. At present, we have no explanation for the observed 20–22-eV resonant peak and the continuous-energy dependence of the CN* desorption yield both shown in Fig. 4.

When investigating neutral-particle desorption, one must consider, in general, the possibility of processes which modify the electronic, vibrational, or rotational states of the escaping primary desorbate. The possible secondary processes which may affect CN* emission are the following: (1) gas-phase excitation of desorbed grounded-state CN, (2) gas-phase dissociation of desorbed alkali-metal CN, and (3) gas-phase neutralization and excitation of desorbed CN^+. In this study, the neutral CN radicals are emitted in excited states with the excitation energy being greater than 3 eV. There are no electrons at the surface energetically available for modification into such a highly excited state except primary beam electrons or secondary electrons. In the modification by primary or secondary electrons, the primary desorption yield is expected to be proportional to the incident electron current and, in addition, the energetic source of modification is also proportional to the current. Thus, the yield of excited CN* should be a quadratic function of the current. This expectation is similar to that made by Walkup, Avouris, and Ghosh.[35] They observed a quadratic behavior of yield versus current for excited Na* formation from NaCl surfaces under electron bombardment. Based on the "quadratic" function, they proposed that excited sodium atoms are produced by the secondary electron excitation of ground alkali-metal atoms thermally desorbed from alkali-metal halide surfaces. However, the desorption yield of CN* as a function of electron current has been studied[33] in the 0.1–10-μA low-current range. The function is linear at the beginning and then tends to saturate at higher currents, since the total amount of CN concentration on the surface is limited by a balance between formation and desorption. The saturation effect may be related to this limited concentration. The measured current dependence at lower currents is not consistent with a quadratic function predicted by secondary processes.

Further evidence against these modifications comes from the measurements of internal energy distributions substrate dependencies, and excitation functions. The impact dissociation of gas-phase alkali-metal CN molecules by secondary electrons can be ruled out by comparing the different energy dependence of the CN* emission yield with the secondary electron yield.[34] Secondary electron excitation of the ground-state CN radical can also be ruled out by contrasting the energy dependencies and the substrate dependencies of the rotational distributions. Walkup, Avouris, and Ghosh[35] suggested that excited alkali-metal atoms are produced by the secondary electron excitation of ground alkali-metal atoms thermally desorbed from high-temperature alkali-metal halide surfaces. This process cannot be responsible for excited CN desorption experiments performed at 60 K since it is impossible to produce thermal desorption of ground-state alkali-metal atoms at such low temperatures. In addition, we observed that the desorption yield is even higher at 60 K than at 300 K. The evidence overwhelmingly suggests that the observed ESD and PSD of excited CN follows a direct electronic bond-breaking process.

B. Rotation mechanisms

As in the desorption process discussed above, the rotational state populations of molecules will depend on the initial bonding state, and on the evolution through an antibonding state to the free state. Despite the lack of experimental data about molecular rotation following electronic interactions between molecules and surfaces, some theoretical studies have been attempted. Briefly, some workers have explained rotational distributions arising from desorbed molecules due primarily to ground-state potential surfaces,[6,7,8] while others attribute the distribution to the repulsive-state potential surface.[9,10] In this work, we suggest a quantum description of desorption and rotation in which the angular momentum may arise both from the initial wave function in the ground state and from the time evolution of the wave functions in the excited state as the molecule is ejected from the surface. In Fig. 11 we illustrate schematically the constraints imposed by a solid surface upon the rotational motion of a molecular adsorbate and relaxation of this constraint as the adsorbate leaves the surface.

At zero temperature, the potential surface in the ground state completely determines the initial wave function. Let Z be the distance along the surface normal of the center of mass of a CN molecule from the surface, θ be the angle that the CN bond makes with the surface normal, and $V(Z,\theta)$ be the potential surface which is a function of Z and θ (to simplify our description, we con-

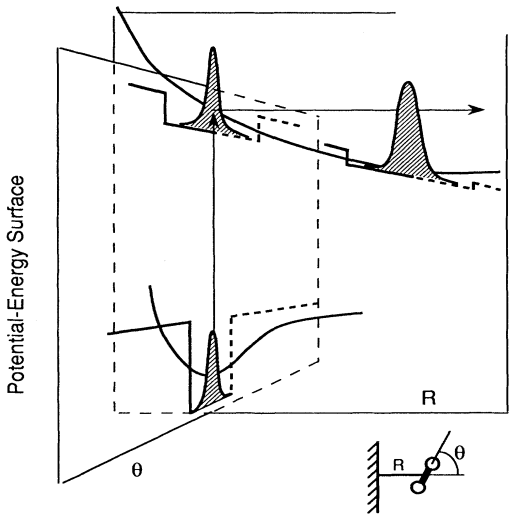

FIG. 11. Scheme of potential surfaces of a CN–alkali-metal system in ground and excited states, the transition between the two states, and the angular localization of the wave function in each state. R is the distance between the surface and the center of mass of the molecule, and θ is the molecular angle relative to surface normal direction. The square wells demonstrate that the potentials vary with angle, and curve potentials vary with distance. The angular parts of the wave functions in each state vary with angle.

sider a cylindrically symmetric system which is φ independent). Initially in the ground state, the Z-dependent potential restricts the CN molecule from moving away from surface and the θ-dependent potential (shown in Fig. 11 as a square potential) restricts the volume in which the molecule rotates (hinders the rotational freedom of the molecule). Thus, the angular part $\phi(\theta,\varphi)$ of the initial wave function may be highly localized.

Electron or photon bombardment of the surface leads to excitation from the bonding state to an antibonding state. Gadzuk and co-workers[6,7] explained rotational distributions based on a transition from a hindered rotor to a free rotor, where the angular distribution is unaffected by the time evolution in the repulsive state. In their model, a rigid dumbbell executes free rotations within a conical domain bounded at some critical pole angle θ by an infinitely repulsive wall. The wall is suddenly switched off by the electronic transition, resulting in a nonequilibrium population of free rotational states due to the conversion of initial zero-point kinetic energy into free rotational energy about the rotor center of mass. In this case, the rotational state distribution is given by a sum of rotational Franck-Condon factors between free-rotor wave function and hindered-rotor wave function. The angular momentum (rotational distribution) can be viewed as a direct measurement of the ground-state potential surface.

In the picture of a transition from a hindered rotor to an approximately free rotor, the zero-point kinetic energy of the hindered rotor is converted to free rotational energy. This energy is greater than the thermal energy, especially in the low-temperature range. As a result, for a strongly hindered rotor, the rotational distribution is independent of the substrate temperature. In fact, our experimental results show that the rotational distributions of desorbed CN* are independent of substrate temperature in the 60- to 300-K range. This indicates that the ground-state hindering potential surface is important in determining the rotational distribution for strongly bonded systems such as alkali-metal (CN).

The potential-energy surface in the excited state determines the time evolution of the initial wave function. In a study of rotational distributions in molecular scattering from surfaces, an angle-dependent potential surface is used by Barker, Kleyn, and Auerbach[36] to analyze the rotational spectrum, displayed by the molecules leaving the surface. Rotation following DIET is similar to the second half of a scattering process. Recently, the work of Hasselbrink[9] and Krempl[10] explained the final rotational distribution in terms of the potential-energy surface in the repulsive state. In these classical models, the anisotropy of the potential results in a net torque exerted on the molecule. Such a torque will influence the molecular rotation. Note that there are obvious differences between full scattering and half scattering (DIET). In full scattering the initial state consists of incoming wave functions. For this case, there is no constraining potential or corresponding steady-state solution to Schrödinger's equation. Even though the initial states are very different, the time evolution of the wave functions as the molecules leave the interaction is the same for full scattering and DIET. This difference is apparent in the experimental data where in the molecular scattering experiments rotational distributions are strongly dependent on the incident energy and the angle, while in DIET rotational distributions depend only on the parent surface bond.

Clearly, both the ground-state potential surface, which determines the initial wave function, and the repulsive-state potential surface, which provides the torque, can affect the molecular rotation of desorbed molecules. The question becomes which effect is dominant in determining the final rotational distribution. For a system where the adsorbate is weakly bonded to the surface, as in the case of Hasselbrink treated, the repulsive-state torque may be critical in determining the rotational distribution; however, for the case where the molecules are strongly chemisorbed on the surface, such as the alkali-metal CN system, the initial distribution may be crucially important in determining the final rotational distribution.

As a result of the above discussions, the final-state rotational populations are determined by the interaction of the parent adsorbed molecules with the surface since this determines both the ground-state and excited-state potentials. This qualitative prediction is consistent with the quantitative experimental observation in this work that the rotational distribution of desorbing CN* is systematically correlated to the alkali-metal component of the substrate. The substrate selectivity of rotational distributions strongly indicates that our spectra are characteristic of the CN–alkali-metal interaction alone. It seems clear that since interactions of CN^- with lighter alkali metals are stronger than those with the heavier ones (as reflected by, for example, the gas-phase heats of formation[37]) these stronger interactions should be translated into higher

rotational-vibrational energies as well as enhanced kinetic energies when the CN^- surface interaction is disrupted.

C. Extraction of the angular-dependent potential surfaces

In this discussion, we will make the argument that the measured rotational spectra give information on potential functions of adsorbed CN interacting with alkali-metal surfaces. Strictly speaking, we cannot determine the potential surface because we do not have additional data such as the orientation of the CN adsorbate with respect to the surface normal. However, we still can discuss the substrate-dependent features of the potential surfaces from the rotational spectra of desorbing CN*, based on the following assumptions: (1) the surface-CN system obeys a cylindrical symmetry about the normal independent of orientation, and (2) the hindered-rotor-to-free-rotor model is valid for the desorption of CN from the alkali-metal surface. The logical steps leading from knowledge of the rotational spectra to a determination of the angular-dependent potential surfaces are the following: First, we construct a parametrized model potential function. Then we solve the initial wave function from the Schrödinger equation with this potential and calculate a rotational distribution utilizing the hindered-rotor-to-free-rotor model. Finally, we determine the parameters of the potential function by fitting the calculated rotational distribution to the measured rotational distribution.

In this treatment, the principal effect of the surface is to hinder or restrict the motion of the adsorbed molecule, or put in another way, restrict the volume in which the molecule rotates. These effects can be described by the standard angular part of the Schrödinger equation,

$$\left\{\frac{1}{\sin\theta}\frac{\partial}{\partial\theta}\left[\sin\theta\frac{\partial}{\partial\theta}\right]+\frac{1}{\sin^2\theta}\frac{\partial^2}{\partial\varphi^2}+\frac{2I}{\hbar^2}[E-V(\theta,\varphi)]\right\}\psi^{\text{hin}}(\theta,\varphi)=0\ , \quad (3)$$

where the quantity I is the molecule's moment of inertia with respect to its center of rotation, θ and φ are as defined in the above section, E is the ground-state zero-point energy, and V is the potential energy of interaction with the surface. The hindering potential results in an angular localization of the initial wave function solved from Eq. (3).

We apply the hindered-rotor-to-free-rotor model, i.e., the sudden approximation, proposed by Gadzuk and coworkers, to our discussion.[6,7] This model is based on the argument that if desorption is induced by a fast process, such as electron or photon bombardment, the molecule is ejected from the surface so rapidly that its wave function is not altered. When the molecule is quickly desorbed from the surface, the molecule becomes a free rotor, which is described by a set of spherical harmonics: $\{Y_{L,m}(\theta,\varphi)\}$. The probability of ending up in the Lth free-rotor state is just a sum of rotational Franck-Condon factors between the initial wave function and $Y_{L,m}(\theta,\varphi)$,

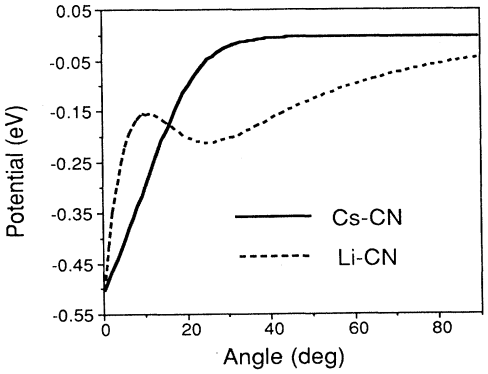

FIG. 12. The potential energies resulting from the least-squares fit as a function of angles for: Li-CN (solid line) and Cs-CN (dashed line).

$$R(L)=\sum_m|\langle Y_{L,m}(\theta,\varphi)|\psi^{\text{hin}}(\theta,\varphi)\rangle|^2\ . \quad (4)$$

where $R(L)$ is the rotational intensity in Lth state. We restrict our treatment to the case for which $m=0$ in the initial system. This is a reasonable assumption for the case of a cylindrically symmetric system with a low substrate temperature.

We modeled the potential function as a combination of two exponential functions with respect to the rotational angle with three parameters (θ_1,θ_2,V_0),

$$V(\theta)=-V_0\frac{e^{-\theta/\theta_1}+Ce^{-\theta/\theta_2}}{1+C}\ , \quad (5)$$

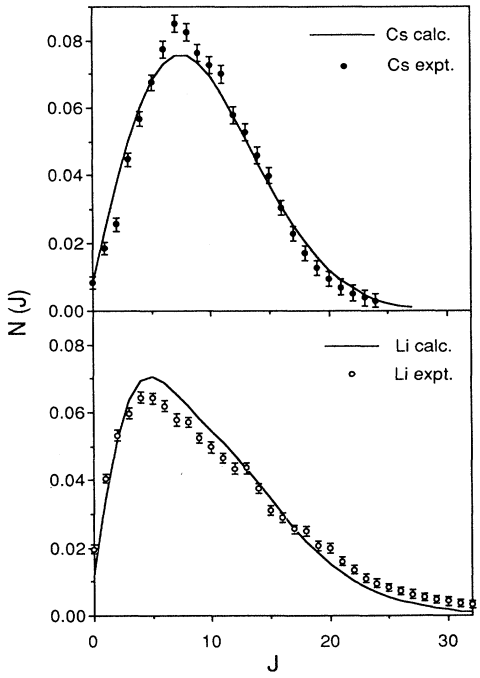

FIG. 13. Comparisons of the calculated rotational distribution with measured distribution: (a) for CN* desorbed from the Li-metal surface, and (b) for CN* desorbed from the Cs-metal surface.

where C is a smoothing function with respect to the two exponential functions given by $C=e^{-10(\theta-15.5)}$. The parameters of the potential function are determined by a least-squares fit of a calculated rotational distribution to a measured rotational distribution. Figure 12 shows the resulting potential functions of CN corresponding, respectively, to the lithium-metal and cesium-metal surfaces; Fig. 13 shows the calculated rotational distributions for the same systems. The fitted parameters are $\theta_1=5.0$, $\theta_2=36.0$, and $V_0=0.5$ eV for the Li-CN system, and $\theta_1=30.0$, $\theta_2=6.5$, and $V_0=0.5$ eV for the Cs-CN system. The parameters in the smoothing function also fall out from the least-squares fit. Our calculations indicate that the smoothing function and its parameters only weakly affect the least-squares fits.

The method used for solving the one-dimensional Schrödinger equation is similar to the Numerov algorithm method, developed by Cooley.[38,39] This method is developed for a diatomic potential well in which the reaction coordinate is the variable of the well. We modified this method by postulating a potential well in which the rotational angle of the molecule is the variable. This method includes calculating the inward and outward wave functions divided by a match angle where the energy E is equal to the potential energy. The computer program arrives at an energy with which the values and the differentials of the inward and outward functions are equal. Then, the resulting energy is the eigenenergy. In our discussion, the energy of the ground state is understood to be the zero-point energy. The breaking of the adsorbate-surface bond releases this zero-point energy to the rotational energies in the free rotor.

As shown in Fig. 12, potential functions depend strongly on the substrate. The potential well for lithium metal in the low-angle regime exhibits a very small full width at half maximum with nonmonotonic behavior in the large angle regime. The full width at half maximum of the potential well for cesium is significantly larger than that of the lithium metal. Our calculations also show that the initial wave function for the lithium-CN system is more localized in the small-angle region than that for cesium and that the zero-point energy for lithium is larger than that for cesium. Thus, more energy is transferred into the excited rotational states for a lithium-metal surface than those for a cesium-metal surface.

As shown in Fig. 13, the calculated rotational distributions do not exactly match the experimental findings. This may indicate that the influence of the excited-state potential surface needs to be considered in calculating the final rotational distributions. The initial wave function, which is determined from the ground-state potential surface, can be modified by the excited-state potential surface. Then, the modified initial wave-function changes the rotational distribution. With consideration of the excited potential surface, the minor well in the large angle regime of the extracted potential of the lithium-CN system may not exist. Clearly, even taking into account the excited potential surfaces, our argument that the measured rotational spectra give information on the relevant potential functions is still valid since the excited-state potential surfaces are also substrate dependent.

VI. CONCLUSIONS

We have reported measurements of the systematic substrate dependence of rotational distributions of excited molecules following electron- and photon-stimulated desorption. Rotational distributions of desorbing excited CN have been measured on LiF, NaF, NaCl, KCl, KBr, CsI, lithium-, sodium-, potassium-, and cesium-metal surfaces, in the surface temperature range of 60–300 K, at 100- and 400-eV electron energies, and for different radiation sources: electron and synchrotron radiation. The results show that rotational distributions of excited CN following ESD and PSD exhibit nonthermal features that are systematically correlated to the alkali-metal component of the substrate, and are independent of surface temperature, incident energy, type of radiation, and halide component of the substrate.

A quantum description of the rotational distributions must ultimately include both the initial wave function in the ground state and the time evolution of the wave functions in the excited state as the molecule is ejected from the surface. Based on a model which assumes a transition from a hindered rotor to a free rotor, the angular-dependent interaction-potential surfaces are extracted from the measured rotational distributions. The extracted potential surfaces are shown to be strongly substrate dependent.

The photon-energy dependence of desorbed CN* has been measured for KCl, potassium-metal, and lithium-metal surfaces. On the potassium-related surface, the measurements show resonant thresholds at 16 and 20 eV, and on the lithium-metal surface, resonant thresholds at 16 and 22 eV. The 16-eV threshold suggests a 4σ-electron ionization of ionically bonded CN with the alkali-metal surface resulting in antibonding between the alkali-metal ion and neutral CN in the B excited state. These resonant energies suggest a direct electronic bond-breaking mechanism, which does not involve core-level electronic states.

The data reveal that important features of the rotational distributions of excited molecules arising from ESD and PSD differ radically from thermal-desorption and momentum-transfer data. These unique substrate-dependent rotational spectra suggest that molecular rotational distributions from these DIET processes are determined by direct electronic bond breaking and reflect the characteristic of the CN–alkali-metal interaction exclusively.

ACKNOWLEDGMENTS

The authors thank Joel Tellinghuisen and John Tully for helpful discussions and the staff of the Synchrotron Radiation Center for their support. This research was sponsored in part by the Air Force Office of Scientific Research (AFOSR) under Contract No. AFOSR-90-0030, by the Office of Naval Research under Contract No. N00014-87-C-0146, and by NASA under Contract No. NAS8-37744.

*Present address: Oak Ridge National Laboratory, P. O. Box 2008, MS 6142, Oak Ridge, TN 37831-6142.
†Present address: Biosym. Technologies, Inc., 10065 Barnes Canyon Rd., San Diego, CA.

[1]A. R. Burns, Phys. Rev. Lett. **55**, 525 (1985).
[2]Steven A. Buntin, Lee J. Richter, Richard R. Cavanagh, and David D. King, Phys. Rev. Lett. **61**, 1321 (1988).
[3]F. Budde, A. V. Hamza, P. M. Ferm, G. Ertl, D. Weide, P. Andresen, and H.-J. Freund, Phys. Rev. Lett. **60**, 1518 (1988).
[4]E. Hasselbrink, S. Jakubith, S. J. Sibener, M.Wolf, A. Cassuto, and G. Ertl, J. Chem. Phys. **92**, 3154 (1990).
[5]*Desorption Induced by Electronic Transitions—DIET I,* edited by N. H. Tolk, M. M. Traum, J. C. Tully, and T. E. Madey (Springer, New York, 1983); *Desorption Induced by Electronic Transitions—DIET II,* edited by M. Brenig and D. Menzel (Springer, New York, 1985); *Desorption Induced by Electronic Transitions—DIET III,* edited by M. L. Knotek and R. H. Stulen (Springer, New York, 1988); *Desorption Induced by Electronic Transitions—DIET IV,* edited by G. Betz and P. Varga (Springer, New York, 1990).
[6]J. W. Gadzuk, Uzi Landman, E. J. Kuster, C. L. Cleveland, and R. N. Barnett, Phys. Rev. Lett. **49**, 426 (1982); J. Electron. Spectrosc. Relat. Phenom. **30**, 103 (1983).
[7]Uzi Landman, E. J. Kuster, C. L. Cleveland, R. N. Barnett, and J. W. Gudzuk, Phys. Rev. B **29**, 4313 (1984).
[8]A. R. Burns, E. B. Stechel, and D. R. Jennison, Phys. Rev. Lett. **58**, 250 (1987).
[9]E. Hasselbrink, Chem. Phys. Lett. **170**, 329 (1990).
[10]Stefan Krempl, Surf. Sci. **259**, 183 (1991).
[11]D. A. Mantell, R. R. Cavanagh, and D. S. King, J. Chem. Phys. **84**, 1531 (1986); R. R. Cavanagh and D. S. King, Phys. Rev. Lett. **47**, 1829 (1981).
[12]David S. Y. Hsu, Mark A. Hoffbaner, and M. C. Lin, Surf. Sci. **184**, 25 (1987).
[13]Greg O. Sitz, Andrew C. Kummel, and Richard N. Zare, J. Chem. Phys. **89**, 2558 (1989).
[14]B. H. Choi, Z. B. Guvenc, and N. L. Liu, Phys. Rev. B **42**, 3887 (1990).
[15]D. Weide, P. Audresen, and H.-J. Freund, Chem. Phys. Lett. **136**, 106 (1987).
[16]Jun Xu, Royal Albridge, Alan Barnes, Menfred Riehl-Chudoba, Akiro Ueda, Norman Tolk, Dwight Russell, and Paul Wang, Surf. Sci. **162**, 185 (1992).
[17]Jun Xu, Alan Barnes, and Norman Tolk, J. Vac. Sci. Technol. A **10**, 2216 (1992).
[18]N. G. Stoffel and P. D. Johnson, Nucl. Instrum. Methods Phys. Res. A **234**, 230 (1985).
[19]N. H. Tolk, L. C. Feibelman, J. S. Kraus, R. J. Morries, M. M. Traum, and J. C. Tully, Phys. Rev. Lett. **49**, 812 (1982).
[20]Jun Xu, Marcus H. Mendenhall, and Joel Tellinghuisen, J. Chem. Phys. **93**, 5281 (1990).
[21]M. Szymonski, J. Ruthowski, A. Poradzisz, Z. Postawa, and Jorgensen, *Desorption Induced by Electronic Transitions—DIET II,* edited by W. Brenig and D. Menzel (Springer, New York, 1985), p. 160; P. Wurz and C. H. Becher, Surf. Sci. **224**, 559 (1989).
[22]G. Roy, G. Singh, and T. E. Gallon, Surf. Sci. **152/153**, 1042 (1985).
[23]K. L. Tsang, C. H. Zhang, and T. A. Callcott, Phys. Rev. B **35**, 8374 (1987).
[24]H. Nakagawa, T. Deguchi, H. Matsumoto, T. Miyanaga, M. Fujita, K. Fukui, E. Ishiguro, I. H. Munro, T. Kato, and M. Watanabe, J. Phys. Soc. Jpn. **58**, 2605 (1989).
[25]M. Watanabe, H. Nakagawa, T. Miyanaga, H. Matsumoto, M. Fujita, and K. Fukui, Phys. Scr. **31**, 154 (1990); J. Lumin. **48/49**, 811 (1991).
[26]R. Engelman, Jr., J. Mol. Spectrosc. **49**, 106 (1974).
[27]R. Engleman, Jr., J. Mol. Spectrosc. **49**, 106 (1974).
[28]D. Menzel and R. Gomer, J. Chem. Phys. **41**, 3311 (1964).
[29]P. A. Redhead, Can. J. Phys. **42**, 886 (1964).
[30]P. E. S. Wormer and J. Tennyson, J. Chem. Phys. **75**, 1245 (1981); J. Tennyson and P. E. S. Wormer, Chem. Phys. Lett. **89**, 223 (1982).
[31]Yihong Yang and Fritz Luty, Phys. Rev. Lett. **51**, 419 (1983).
[32]Zhou Xu-Yan, Shi Dan-Hua, and Cao Pei-Lin, Surf. Sci. **223**, 393 (1989).
[33]Jun Xu, Ph.D. thesis, Vanderbilt University (1991).
[34]P. Bunton, R. Hugland, D. Liu, and N. Tolk, Surf. Sci. **243**, 227 (1991).
[35]R. E. Walkup, Ph. Avouris, and A. P. Ghosh, Phys. Rev. Lett. **57**, 2227 (1986); Phys. Rev. B **36**, 4577 (1987).
[36]J. A. Barker, A. W. Kleyn, and D. J. Auerbach, Chem. Phys. Lett. **97**, 9 (1983).
[37]M. W. Chase, Jr., C. A. Davies, J. R. Downey, Jr., D. J. Frurip, R. A. McDonald, and A. N. Syverud, J. Phys. Chem. Ref. Data **14**, 1 (1985).
[38]J. W. Cooley, Math. Comput. **15**, 363 (1961).
[39]J. Tellinghuisen, Int. J. Quantum Chem. **34**, 401 (1988).